

HPC: Hierarchical Progressive Coding Framework for Volumetric Video

Zihan Zheng*
Shanghai Jiao Tong
University
Shanghai, China
1364406834@sjtu.edu.cn

Houqiang Zhong*
Shanghai Jiao Tong
University
Shanghai, China
zhonghouqiang@sjtu.edu.cn

Qiang Hu†
Shanghai Jiao Tong
University
Shanghai, China
qiang.hu@sjtu.edu.cn

Xiaoyun Zhang
Shanghai Jiao Tong
University
Shanghai, China
xiaoyun.zhang@sjtu.edu.cn

Li Song
Shanghai Jiao Tong
University
Shanghai, China
song_li@sjtu.edu.cn

Ya Zhang
Shanghai Jiao Tong
University
Shanghai, China
ya_zhang@sjtu.edu.cn

Yanfeng Wang
Shanghai Jiao Tong
University
Shanghai, China
wangyanfeng@sjtu.edu.cn

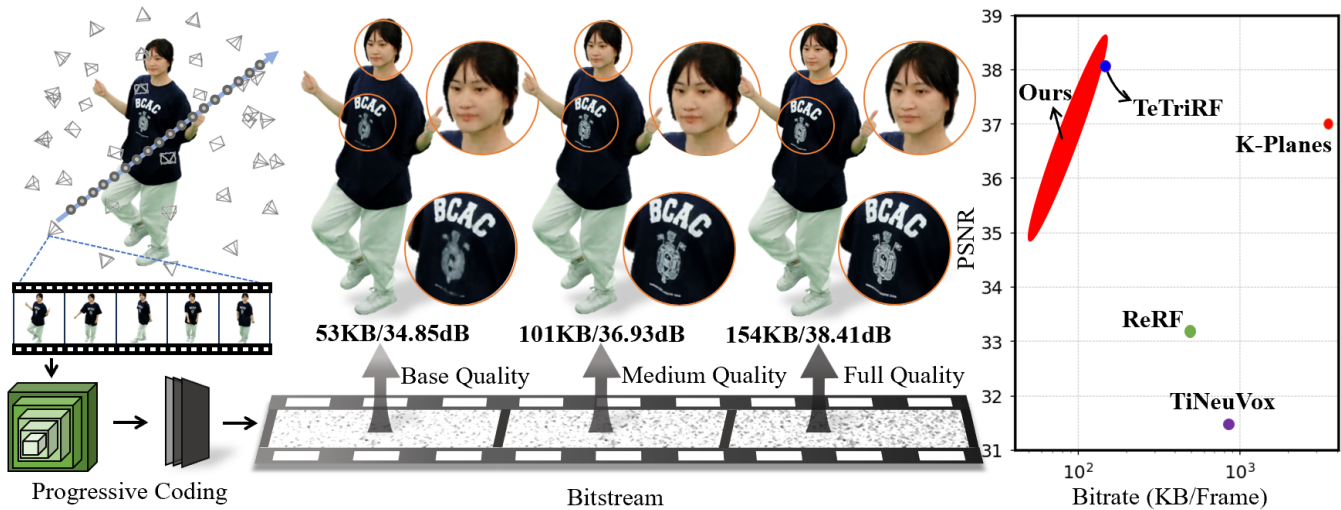


Figure 1: Overview. With hierarchical representation (left), our HPC progressively encodes the volumetric video into a scalable bitrate bitstream using a single model, enabling different quality reconstructions (e.g., base quality 34.85dB@53KB, medium quality 36.93dB@101KB, full quality 38.41dB@154KB). The RD performance (right) still outperforms those fixed-bitrate methods (e.g., ReRF[65], TeTriRF[71]).

Abstract

Volumetric video based on Neural Radiance Field (NeRF) holds vast potential for various 3D applications, but its substantial data volume poses significant challenges for compression and transmission. Current NeRF compression lacks the flexibility to adjust

*Authors contributed equally to this work.

†Corresponding author.

Permission to make digital or hard copies of all or part of this work for personal or classroom use is granted without fee provided that copies are not made or distributed for profit or commercial advantage and that copies bear this notice and the full citation on the first page. Copyrights for components of this work owned by others than the author(s) must be honored. Abstracting with credit is permitted. To copy otherwise, or republish, to post on servers or to redistribute to lists, requires prior specific permission and/or a fee. Request permissions from permissions@acm.org.

MM'24, October 28 - November 1, 2024, Melbourne, Australia.

© 2024 Copyright held by the owner/author(s). Publication rights licensed to ACM.

ACM ISBN 979-8-4007-0686-8/24/10

<https://doi.org/10.1145/3664647.3681107>

video quality and bitrate within a single model for various network and device capacities. To address these issues, we propose HPC, a novel hierarchical progressive volumetric video coding framework achieving variable bitrate using a single model. Specifically, HPC introduces a hierarchical representation with a multi-resolution residual radiance field to reduce temporal redundancy in long-duration sequences while simultaneously generating various levels of detail. Then, we propose an end-to-end progressive learning approach with a multi-rate-distortion loss function to jointly optimize both hierarchical representation and compression. Our HPC trained only once can realize multiple compression levels, while the current methods need to train multiple fixed-bitrate models for different rate-distortion (RD) tradeoffs. Extensive experiments demonstrate that HPC achieves flexible quality levels with variable bitrate by a single model and exhibits competitive RD performance, even outperforming fixed-bitrate models across various datasets.

CCS Concepts

• **Information systems** → **Multimedia streaming**.

Keywords

Volumetric Video, Dynamic NeRF, Progressive Coding, End-to-end Optimization

ACM Reference Format:

Zihan Zheng, Houqiang Zhong, Qiang Hu, Xiaoyun Zhang, Li Song, Ya Zhang, and Yanfeng Wang. 2024. HPC: Hierarchical Progressive Coding Framework for Volumetric Video. In *Proceedings of the 32nd ACM International Conference on Multimedia (MM '24)*, October 28–November 1, 2024, Melbourne, VIC, Australia. ACM, New York, NY, USA, 11 pages. <https://doi.org/10.1145/3664647.3681107>

1 Introduction

Volumetric video captures dynamic 3D scenes, which allows users to freely select their viewing angles for a unique and immersive exploration experience. With its powerful 3D realism and interactive capabilities, volumetric video holds vast potential for 3D applications such as virtual reality, telepresence, sports broadcasting, remote teaching, and beyond. Therefore, volumetric video is considered a cornerstone for the next generation of media.

Recent advances in Neural Radiance Field (NeRF)[46] facilitate dynamic scene rendering for photorealistic volumetric video generation. Some methods[16, 37, 48, 52] utilize deformation fields to track voxel displacements relative to a canonical space, capturing motion information in volumetric video. However, their reliance on canonical space limits their effectiveness in sequences with large motion or topological changes. Other methods [16–18, 20, 22, 32, 70, 72] extend the radiance field to 4D spatio-temporal domains or introduce temporal voxel features, using a single neural network to fit 4D scenes and directly train on multi-view video data for high-quality temporal reconstruction. These methods effectively capture the dynamic details of scenes, but the substantial data volume poses significant challenges for transmitting volumetric video.

Several methods [15, 51, 55, 59, 65, 66, 71] have been developed to compress explicit features of dynamic NeRF for efficiently storing and transmitting volumetric video. ReRF[65] employs a compact motion grid and residual grid for representation, followed by traditional image encoding techniques to further reduce redundancy. TeTriRF[71] utilizes a three-plane decomposition of the representation and traditional video encoding methods, yielding improved results. However, they rely on traditional image/video encoding techniques and fail to jointly optimize the representation and compression of the radiance field, resulting in the loss of dynamic details and reduced compression efficiency. Additionally, they lack the flexibility to adjust video quality and bitrate within a single model for various network and device capacities. For achieving different bitrates, they require re-training and storing each model separately, resulting in large storage cost.

In this paper, we propose HPC, a novel hierarchical progressive volumetric video coding approach achieving variable bitrate using a single model. Our HPC improves coding efficiency and enables progressive variable bitrate streaming of data by being able to scale the quality to available bandwidth or desired level of detail (LOD), see Fig. 1. Our key idea is to use multi-resolution feature

grids which can be truncated at any level to achieve adaptive bitrate and quality. We hence introduce a hierarchical representation with multi-resolution residual feature grids to fully utilize feature relevance between consecutive frames. The feature grids of the representation are then sequentially quantized and entropy encoded to further reduce redundancy.

Moreover, we present an end-to-end progressive training scheme to jointly optimize both the hierarchical representation and compression, significantly enhancing the rate-distortion (RD) performance. Specifically, considering the non-differentiability of quantization and entropy encoding during compression, we introduce a method for simulating quantization and estimating bitrate, thus enabling gradient back-propagation. Additionally, we employ a multi-rate-distortion loss function together with a step-by-step training strategy to optimize the entire scheme. Experimental results demonstrate that our HPC achieves variable bitrate by a single model with higher compression efficiency compared to the fixed-bitrate models.

In summary, our contributions are as follows:

- We propose HPC, the first approach to enable progressive volumetric video coding, streaming and decoding. Our HPC achieves flexible quality levels and variable bitrate within a single model, while maintaining competitive RD performance.
- We present an efficient and compact hierarchical representation, which represents volumetric video as a multi-resolution residual radiance field with low temporal redundancy for high efficiency progressive compression.
- We introduce an end-to-end progressive learning approach that jointly optimizes hierarchical representation and compression based on a multi-rate-distortion loss function to enhance RD performance at each layer and overall.

2 Related work

2.1 Neural Scene Representation

NeRF[46] achieves photorealistic synthesis of new viewpoints using an implicit representation. This powerful method has quickly gained attention and has been extensively applied in various domains including pose estimation[10, 34, 64, 82, 83], 3D generative modeling[8, 23, 24, 27, 45], and 3D reconstruction[14, 33, 38, 61, 68, 69, 75]. In tasks involving the synthesis of new viewpoints in static scenes, NeRF-based approaches have recorded significant achievements. Differentiable rendering[10, 34, 49, 64, 82, 83] has demonstrated strong robustness against inaccuracies in camera pose inputs. A range of techniques[4–6, 43, 69] aimed at scene modeling has notably enhanced the quality of NeRF volumetric rendering. Additionally, various dense 3D representations such as octrees[19, 53, 67], multiscale hash tables[47], tensors[9, 60, 77], and mesh assets[11, 21, 54, 56, 75] have been explored to accelerate training and rendering. The breakthroughs achieved by NeRF in static scenes have spurred research into its application in dynamic scenes, laying a solid foundation for further advancements.

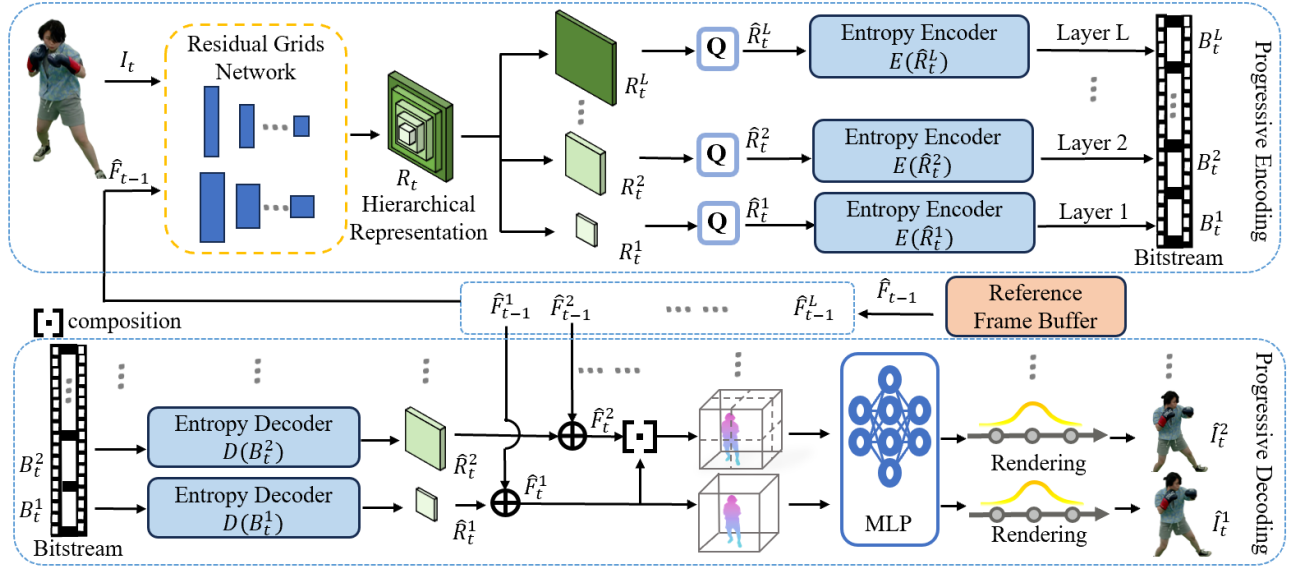


Figure 2: Illustration of our HPC framework. In progressive encoding, residual grids network takes images I_t and previous reconstructed feature grids \hat{F}_{t-1} as input, generates multi-resolution residuals R_t . After quantization Q , the residuals are encoded into a bitstream B_t via entropy encoder E . During progressive decoding, residuals are decoded from the bitstream and then recursively integrates with prior reference grids to recover the current frame features layer by layer.

2.2 Dynamic Radiance Field Representation

Dynamic scenes present significant challenges, particularly when dealing with large motions on new view synthesis. Current advances in Neural Radiance Field (NeRF)[46] promote dynamic scene rendering for photorealistic volumetric video generation. The deformation field methods[16, 32, 48, 52, 59] recover temporal features by warping the live-frame space back into the canonical space, yet struggle with large motions and changes, leading to slower training and rendering. Another category of methods[7, 17, 18, 22, 30, 51, 53, 57, 70, 76, 78] extends the radiance field to 4D spatial-temporal domains, where they model the time-varying radiance field in a higher-dimensional feature space for quicker training and rendering, though at the cost of increased storage needs. Several works[65, 66, 71] adopt the residual radiance field technique by leveraging compact motion grids and residual feature grids to exploit inter-frame feature similarity, achieving favorable outcomes in representing long sequences of dynamic scenes. Our hierarchical representation further integrates the concept of residuals to correct errors and incorporate newly encountered regions, significantly reducing data redundancy. Moreover, this hierarchical representation enables us to implement progressive encoding, enhancing our capability to deliver optimal viewing experiences across varied network conditions and device capabilities.

2.3 NeRF Compression

In recent years, deep learning-based image and video compression methods[1–3, 12, 25, 26, 31, 35, 36, 39–41, 44, 58, 62, 63, 73, 74, 80] have been widely applied, achieving good rate-distortion (RD) performance on 2D videos. Currently, there are some efforts[15, 28, 29, 51, 55] underway to apply compression techniques in the NeRF

domain. Among them, VQRF[29] employs an entropy encoder to compress the static radiance field model, while ECRF[28] maps radiance field features to the frequency domain before applying entropy encoding. Despite their efficacy, these methods are still restricted to static scenes, and lack exploration in dynamic spaces. ReRF[65], VideoRF[66], and TeTriRF[71] focus on dynamic scene modeling, employing traditional image/video encoding techniques for enhanced feature compression and do not simultaneously optimize both the representation and compression of the radiance field, leading to a loss of dynamic details and lower compression efficiency. Similar to approach[79, 81], we have designed a deep learning-based compression method for feature grids which can be optimized with representation and compressed for dynamic scenes, achieving very good RD performance.

3 Method

Our framework, depicted in Fig. 2, is organized into two core segments: hierarchical progressive encoding and hierarchical progressive decoding. The input includes multi-view images I_t along with former reference feature grids. These inputs are processed through a residual grids network, designed to produce residual feature grids at multiple resolutions. These residual features are passed through entropy encoders and transmitted to the decoding side as a bitstream. During the decoding phase, the bitstream is decoded by entropy decoders into multi-resolutions residuals. They are integrated with former reference features to render images at different scales according to various bitrates. This process allows for the adaptive rendering of volumetric video outputs \hat{I}_t , catering to different compression needs and ensuring the high-quality content across varying resolutions. Next, we introduce the details about the

proposed hierarchical progressive encoding in Sec.3.1, consisting of hierarchical representation and entropy encoder, followed by hierarchical progressive decoding in Sec.3.2.

3.1 Hierarchical Progressive Encoding

Hierarchical representation. Recall that the NeRF-based representations map the implicit neural feature to color and density with MLP Φ , where the feature F is determined by sampling position (x, y, z) and view direction \mathbf{d} .

$$(c, \sigma) = \Phi(F(x, y, z, \mathbf{d})) \quad (1)$$

For long-sequence dynamic volumetric videos, our aim is to precisely establish the radiance field for each frame. Transitioning from a static to a dynamic scene highlights a significant challenge in data explosion. The simplistic method of transmitting individual per-frame feature grids F_t for a dynamic scene overlooks the essential aspect of temporal coherence, leading to considerable data redundancy. To mitigate the inefficiency of transmitting the entire radiance field for each frame and capitalize on the sequence's continuity, we segment the video sequence into multiple groups of features (GoFs), with each group comprising N frames. Within these groups, take the first group for example $G_1 = \{F_1, R_2, R_3 \dots R_N\}$, we establish frame-to-frame residuals based on forward references, thus harnessing the inherent temporal coherence and substantially reducing the data required for accurate scene representation. And the feature grid of the frame t can be recursively reconstructed by combining the feature grid of the previous frame with the current frame's residual R_t .

$$F_t = F_{t-1} + R_t \quad (2)$$

We decompose a large feature grid F into L different resolutions to meet the needs for progressive streaming, $F = \{F^l \mid l \in [1, L]\}$. With the increment of the index l , each level of the feature grid F^l increases in resolution and enhances the details captured in the scene. By merging these feature grids from the lowest to the highest resolution, the reconstructed scene can be presented at different levels of precision. This methodology allows for the use of a single model to output features at different bitrates, satisfying the volumetric video viewing experience under various bandwidth conditions. Our multi-resolution residual representation is shown in Fig. 3. Within the GoFs, each group starts with a L -levels full feature grids as reference and follows with L -levels residuals. For frame t , F_t is reconstructed by adding together the residuals and the features from the previous frame at their respective levels. Our hierarchical representation with multi-resolution residual radiance fields, effectively reducing temporal redundancy in extended sequences and offering scalable quality adjustments. This approach tailors the streaming experience to fluctuating network conditions or specific requirements for the level of detail, enhancing both the efficiency and flexibility of volumetric video delivery.

$$F_t = \{F_{t-1}^l + R_t^l \mid l \in [1, L]\} \quad (3)$$

Entropy Encoder. The sparsity of radiance field residual features significantly enhances compression and transmission efficiency. We scale the residuals of each level by the quantization parameter and round it to uint8, thereby substantially reducing

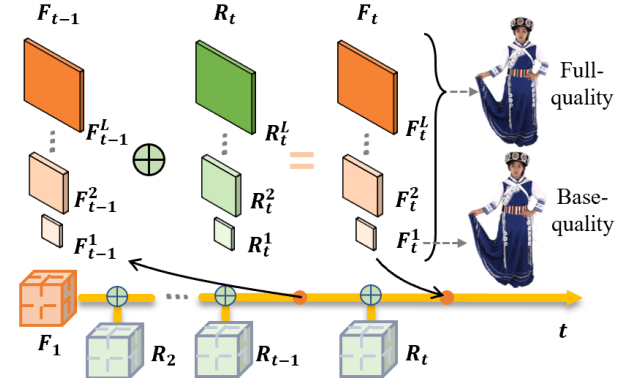


Figure 3: The multi-layered feature grids for subsequent frames F_t can be recursively reconstructed by layer-wise accumulation of residuals R_t .

the volume of data required for an accurate depiction. Following this quantization, the quantized residuals are subjected to compression via a range encoder[42], culminating in the generation of a more compact bitstream B . Notice that the residuals at each level are processed through separate entropy encoders rather than being amalgamated for collective compression. This layered approach ensures the unique statistical properties and predictability of the residuals at each resolution are meticulously accounted for, enabling more effective compression.

$$B_t = \{B_t^l \mid l \in [1, L]\} \quad (4)$$

$$B_t^l = E^l \left(Q(q \cdot R_t^l) - Q \left(q \cdot \min(R_t^l) \right) \right) \quad (5)$$

where E^l is the l -th entropy encoder, and Q represents the quantization operation. In order to facilitate compression into the uint8 format, the data is first converted into non-negative values. The variable q is the quantization parameter. During quantization, data is multiplied by q , effectively expanding the data range and enhancing quantization precision. By adjusting the parameter q , we trade-off between reconstruction quality and model storage.

3.2 Hierarchical Progressive Decoding

Hierarchical Decoding. On the decoding side, the user receives the transmitted bitstream and then decodes it using an entropy decoder to recover the original features. The operation is articulated as follows:

$$\hat{R}_t = \frac{D(B_t) + Q(q \cdot \min(R_t))}{q}, \quad (6)$$

where D is the entropy decoder. Since the data was converted into non-negative values and multiplied by q , we will revert it to its original range during decompression.

In practical scenarios, both the bandwidth available for data transmission and the computational power of decoding devices may be limited, insufficient to process all data. However, given that our scene representation is hierarchical, we can adaptively render dynamic scenes with varying effects at the decoding end, tailored to the device's computational capacity. Specifically, by selecting a smaller level l , we can choose to only receive and decode

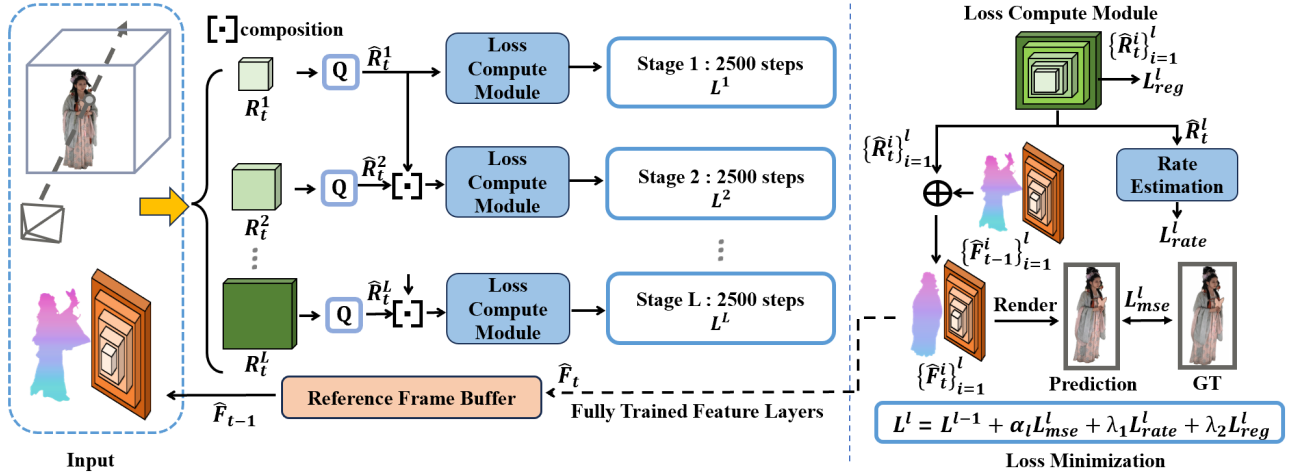


Figure 4: Overview of our hierarchical progressive training. We generate different resolution feature grids R_t^l from current frame images and previous reference feature \hat{F}_{t-1} from buffer. The network trains on the most basic resolution grids, $l = 1$. As training advances, it progressively incorporates higher resolution grids from the next level, while supervising at each layer via the multi-rate-distortion loss L^l . After training is completed, the trained feature grids \hat{F}_t^l are stored in the reference frame buffer.

$\{\hat{F}^i \mid i \leq l\}$ and then render up to that selected resolution, ignoring the remaining higher-resolution $\{\hat{F}^i \mid i > l\}$. This approach facilitates a trade-off between rendering quality and model storage requirements.

We simultaneously transmit bitstream of varying resolutions, enabling the decoder to receive and process these data streams in parallel. Our methodology facilitates the implementation of LOD, progressively enhancing the granularity of scene details over time. This allows for a more efficient and dynamic presentation of complex scenes, aligning with the demands of high-fidelity visualization and real-time processing requirements.

Rendering. After decoding the reconstructed feature grids $\{\hat{F}^l\}$, we can obtain the corresponding color c_i^l and density σ_i^l through Eq.(1). Within a Group of Features (GoF), all frames and all levels of features are decoded and rendered through a global MLP Φ . Then we proceed with volume rendering to obtain the rendering result. By accumulating the colors c_i^l and densities σ_i^l of all sampled points along a ray \mathbf{r} , we can derive the predicted color $\hat{c}^l(\mathbf{r})$ at resolution l for the corresponding pixel:

$$\hat{c}^l(\mathbf{r}) = \sum_i^N T_i (1 - \exp(-\sigma_i^l \delta_i)) c_i^l, \quad (7)$$

where $T_i = \exp(-\sum_{j=1}^{i-1} \sigma_j \delta_j)$, and δ_i denotes the distance between adjacent samples. In this way, we finally get the multi-resolution rendering results.

4 Hierarchical Progressive Training

In this section, we introduce our designed hierarchical progressive training methods, with the training process illustrated in Fig. 4. We train different feature grids progressively, jointly optimizing reconstruction and compression. Our training approach is primarily

divided into two parts: end-to-end joint optimization (Sec.4.1) and progressive training strategy (Sec.4.2).

4.1 End-to-end Joint Optimization

Here, we detail an end-to-end optimization strategy for enhancing compression efficiency by jointly optimizing the representation and compression of HPC. By applying simulated quantization to the feature grids R_t and using an entropy model for bitrate estimation, we facilitate efficient end-to-end training. The objective of end-to-end joint optimization is to minimize the entropy of the radiance field representation while ensuring high reconstruction quality.

Simulated Quantization. Implementing quantization during the compression process significantly reduces the bitrate of feature grids at the expense of some information loss. By incorporating the quantization operation within the training phase, we enhance the model's robustness to the information loss caused by quantization. However, the rounding operation interrupts gradient flow, complicating end-to-end training. To avoid this, we emulate the effects of quantization by introducing uniform noise within the $[-\frac{1}{2}, \frac{1}{2}]$ range, as depicted in Eq.(8), allowing gradient flow to be preserved and supporting end-to-end training.

$$Q(x) = x + u, u \sim U(-\frac{1}{2}, \frac{1}{2}). \quad (8)$$

Rate Estimation. Entropy encoding on quantized feature grids produces a highly compressed bitstream. By incorporating bitrate measurement into the training phase and including it in the loss function, we encourage a distribution of features with lower entropy, effectively imposing a bitrate constraint during network updates. However, entropy encoding disrupts gradient flow, either. To address this, entropy models are introduced during training to estimate the entropy of the grids, representing the compression bitrate's lower bound. These models are capable of approximating

the probability mass function (PMF) for the quantized values \hat{y} of a feature grid by calculating its cumulative distribution function (CDF), as demonstrated in Eq.(9). This approach enables network optimization towards lower bitrates while maintaining compatibility with gradient-based training.

$$P_{PMF}(\hat{y}) = P_{CDF}(\hat{y} + \frac{1}{2}) - P_{CDF}(\hat{y} - \frac{1}{2}). \quad (9)$$

To maintain precision, we refrain from the assumption of any predefined data distribution for the 3D grids. Instead, we construct a novel distribution within the entropy model to closely match the actual data distribution. The entropy model plays a crucial role during training by estimating the size of the compressed bitstream of \mathbf{R}_t^l at resolution l , named \mathcal{L}_{rate}^l , which in turn informs the overall loss calculation.

$$\mathcal{L}_{rate}^l = -\frac{1}{L} \sum_{\hat{y} \in \mathbf{R}_t^l} \log_2(P_{PMF}(\hat{y})) \quad (10)$$

4.2 Progressive Training Strategy

When end-to-end joint optimization is applied to feature grids across all resolutions within an entire scene, superior performance is achieved at the highest level. However, only supervising the overall reconstruction quality and simultaneously training all feature grids cannot ensure optimal results at every layer. In light of these challenges, we introduce our progressive training strategy, growing model with multi-level supervision.

Initially, the network trains only on the most basic resolution grids, $l = 1$. As training progresses, the model integrates higher resolution grids from the next $l + 1$ level, and supervises rendering for each layer of grids. Towards the final phases of training, we intentionally halt training on the low-resolution grids, and rate supervision is also progressively discontinued. This approach encourages the model to focus more on capturing finer details at the highest resolution grid.

Training Objective. The multi-rate-distortion loss function of each stage is defined as:

$$\mathcal{L}^l = \mathcal{L}^{l-1} + \alpha_l \mathcal{L}_{mse}^l + \lambda_1 \mathcal{L}_{rate}^l + \lambda_2 \mathcal{L}_{reg}^l \quad (11)$$

$$\mathcal{L}_{mse}^l = \sum ||\mathbf{c}(\mathbf{r}) - \hat{\mathbf{c}}^l(\mathbf{r})||^2, \quad (12)$$

$$\mathcal{L}_{reg}^l = ||\hat{\mathbf{R}}_t^l||_1, \quad (13)$$

where \mathcal{L}^l is the loss of level l , \mathcal{L}_{mse}^l metrics the difference between the ground truth and the result of different levels of resolution rendered by our framework, measuring the quality of reconstruction. \mathcal{L}_{rate}^l represents the estimated rate derived from $\hat{\mathbf{R}}_t^l$. \mathcal{L}_{reg}^l is the L1 regularization applied to $\hat{\mathbf{R}}_t^l$ of different resolution to ensure temporal continuity and minimize the magnitude of $\hat{\mathbf{R}}_t^l$. The parameter λ_1 is used to balance the rate and distortion, allowing for control over the model size and reconstruction quality. The parameter λ_2 measures the extent of our constraint on $\hat{\mathbf{R}}_t^l$.

5 Experimental Results

5.1 Configurations

Datasets. In this section, we extensively assess our HPC framework on the ReRF[65] and DNA-Rendering[13] datasets. The ReRF dataset

, 1920×2080, includes 74 camera views. We assign 70 for training and the remaining 4 for testing. The DNA-Rendering dataset, 2048×2448, includes 48 views, with 46 used for training and 2 for testing. For fairness, we specify the same bounding box for the same sequence in different comparison experiments.

Setups. In our framework, we specify the number of feature grids, L , as 6. Our experimental setup includes an Intel(R) Xeon(R) W-2245 CPU @ 3.90GHz and an RTX 3090 graphics card. During training, the initial settings are as follows: λ_1 and λ_2 are set to 0.000001, α_6 (for full modeling) is set to 1, and the remaining α_l values are set at 0.25. The maximum number of iterations, *maxiter*, is set to 40,000, with the activation iteration, *actiter*, at 2,500. We utilize six distinct entropy models, each tailored to one of the six different-resolution feature grids. The duration for each GoF is consistently fixed at 20 frames.

5.2 Comparison

To our knowledge, HPC is the first framework for hierarchical progressive volumetric video coding, using a multi-resolution residual radiance field for optimized compression. It achieves variable RD performance through progressive encoding and decoding without additional training or compression. To validate HPC’s effectiveness, we compare it at different resolutions with TiNeuVox[17], K-Planes[18], ReRF[65], and TeTriRF[71] both qualitatively and quantitatively. Figure 5 shows visual results of two sequences, demonstrating HPC’s superiority in model compactness and detail precision.

Besides qualitative experiments, we also conduct a quantitative comparison in terms of Peak Signal-to-Noise Ratio (**PSNR**), Structural Similarity Index (**SSIM**) and model storage as shown in Table 1. Our method shows significant advantages in reconstruction quality and model storage, achieving optimal rate-distortion performance. TiNeuVox[17] performs poorly on long sequences. K-Planes[18] has good reconstruction for known viewpoints but struggles with unknown ones and has a large model size. ReRF[65] has similar model storage to ours, but lower reconstruction quality. TeTriRF[71]’s RD performance is nearly comparable to ours but lacks progressive coding. Unlike ReRF[65] and TeTriRF[71], which require additional training and compression to adjust quality and storage trade-offs,

Table 1: Quantitative comparison against volumetric video encoding methods. We calculate the average PSNR, SSIM, and storage for each frame across all training and testing views separately.

Dataset	Method	Training View		Testing View		Size (MB) [↓]
		PSNR \uparrow	SSIM \uparrow	PSNR \uparrow	SSIM \uparrow	
ReRF	TiNeuVox[17]	31.03	0.964	27.12	0.958	0.81
	K-Planes[18]	37.97	0.985	30.01	0.971	2.99
	ReRF[65]	33.04	0.979	30.88	0.975	0.50
	TeTriRF[71]	38.01	0.987	33.45	0.980	0.14
	Ours	38.38	0.990	33.55	0.981	0.14
DNA-Rendering	TiNeuVox[17]	29.28	0.953	22.19	0.947	0.80
	K-Planes[18]	31.98	0.979	27.81	0.962	3.00
	ReRF[65]	30.20	0.974	29.59	0.972	0.31
	TeTriRF[71]	32.33	0.980	29.48	0.973	0.16
	Ours	32.69	0.983	29.88	0.977	0.15

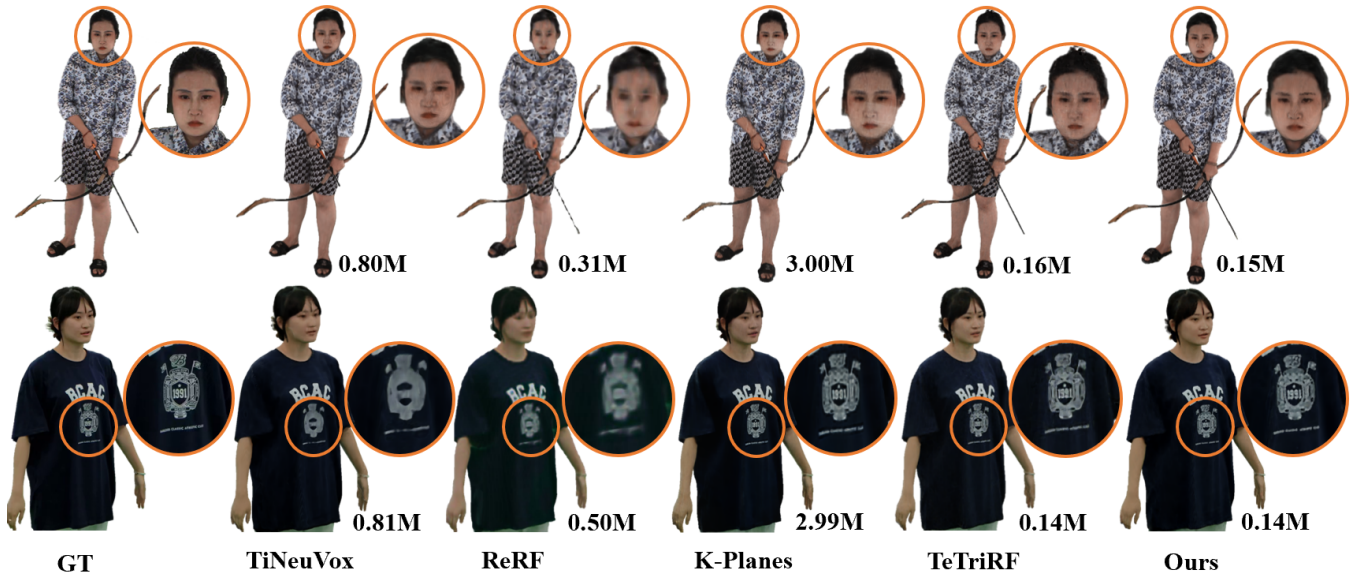


Figure 5: Qualitative comparison against volumetric video coding methods TineuVox[17], K-Planes[18], ReRF[65], TeTriRF[71].

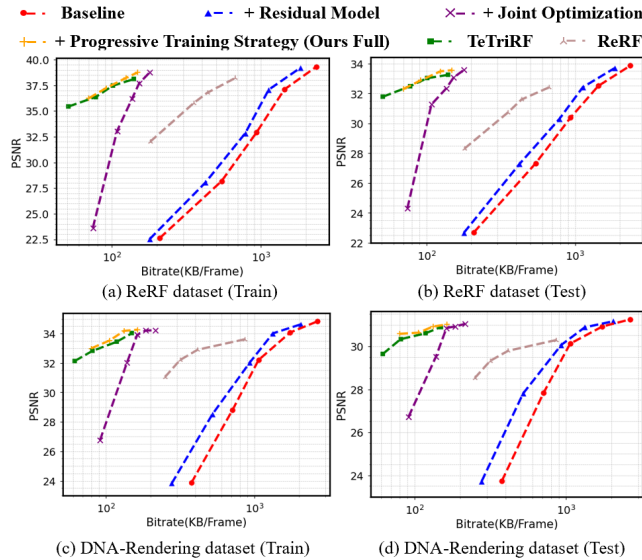


Figure 6: Rate-distortion curves in both the ReRF and DNA-Rendering datasets. Rate-distortion curves not only illustrate the efficiency of various components within our method, but also demonstrate its superiority over ReRF[65] and TeTriRF[71].

our method optimizes this by selecting the number of feature grids during decoding.

Fig. 6 and Table 2 also shows a comparison of RD performance between our HPC, ReRF[65] and TeTriRF[71]. We evaluate these methods using Bjontegaard Delta Bit-Rate (**BDBR**) and Bjontegaard Delta Peak Signal-to-Noise Ratio (**BD-PSNR**)[50]. From Table 2, we can see that on the ReRF dataset, we observe average BDBR

Table 2: The BDBR results of our HPC and TeTriRF[71] when compared with ReRF[65] on different datasets.

Dataset	Method	Training View		Testing View	
		BD-PSNR ↑ (dB)	BDBR ↓ (%)	BD-PSNR ↑ (dB)	BDBR ↓ (%)
ReRF	TeTriRF[71]	6.582	-80.822	4.878	-86.948
	Ours	7.576	-81.523	5.173	-87.946
DNA-Rendering	TeTriRF[71]	5.516	-80.575	4.037	-88.682
	Ours	5.633	-82.463	4.398	-89.192

reductions of 81.523% and 87.946% for training and testing views, respectively. Similarly, on the DNA-Rendering dataset, the average BDBR saving is 82.463% and 89.192% for training and testing views, respectively. Fig. 6 also demonstrates the superior RD performance of our method. Our method obviously performs better than ReRF[65] and have a slightly better result with TeTriRF[71]. However, all of them need to train multiple fixed-bitrate models for different rate-distortion tradeoffs. In contrast, Our method supports achieving multiple RD performances with a single compression and training process.

In additional, we evaluate the computational complexity of HPC at different quality levels, as detailed in the Table 3. Our decoding and rendering time gradually increases as reconstruction quality improves due to our use of higher-dimensional features to capture additional scene details, resulting in increased data volume and complexity required for decoding and rendering. Our method achieves shorter decoding and rendering times at base and medium reconstruction qualities, significantly outperforming TeTriRF[71] and remaining competitive with ReRF[65]. At full reconstruction quality, we achieve computational performance comparable to TeTriRF.

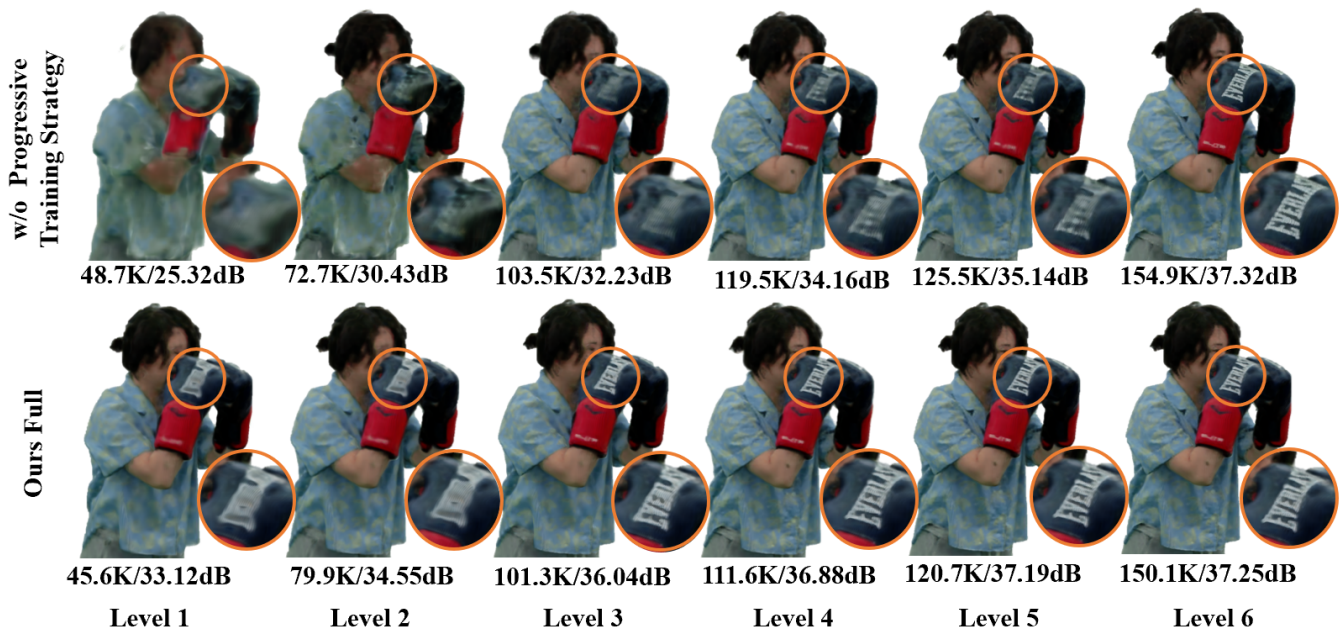


Figure 7: The results of our full method in comparison to approaches without progressive training strategy. With the progressive training strategy, our HPC achieves flexible quality levels at variable bitrate using a single model.

Table 3: Computational complexity of our HPC at different quality levels in compression to ReRF[65] and TeTriRF[71].

Time	TeTriRF [71]	ReRF [65]	Ours		
			Base Quality	Medium Quality	Full Quality
Decode(ms)	101	55	22	43	121
Render(ms)	120	58	56	72	109

5.3 Ablation Studies

We conduct three ablation studies to validate the effectiveness of each component in our method. As a baseline, we opt for quantization and entropy encoding on the hierarchical representation and incrementally add each component under test to the baseline. Our primary focus lies on the dynamic residual model, end-to-end joint optimization, and progressive training strategy. In the first ablation study, we build on the baseline by adding the dynamic residual model. The second ablation study extends the first by incorporating an end-to-end joint optimization of the NeRF reconstruction and compression. Finally, in the third ablation study, which represents our full method, we further enhance the second study’s setup by integrating the progressive training strategy.

The ablation study results are shown in Fig. 6. We adjusted the axis scales for clarity. Using the dynamic residual model, we represent non-keyframe features with small residual grids, significantly reducing the overall model size. Joint optimization enhances rate-distortion performance and reduces storage while hardly affecting the reconstruction quality. Moreover, it offers advantages in terms of reconstruction quality over the baseline when we don’t utilize all feature grids. Our progressive training strategy further decreases model size and improves robustness, enabling low-resolution grids

to convey structural information effectively, whose importance can also be seen in Fig. 7 as HPC maintains excellent rendering quality across each level of result. Overall, the ablation studies highlight the critical roles of the dynamic residual model, joint optimization, and progressive training strategy.

6 Conclusion

In this paper, we propose HPC, the first progressive volumetric video coding approach, enabling flexible and effective scaling between quality and bitrate. HPC introduces a highly compact hierarchical representation with a multi-resolution residual radiance field to effectively leverage feature relevance between frames and generate different levels of detail. Furthermore, HPC employs an end-to-end progressive training scheme to jointly optimize the hierarchical representation and compression based on a multi-rate-distortion loss function, significantly improving RD performance of each level and overall. Experimental results show that HPC achieves variable bitrate using a single model and outperforms the state-of-the-art fixed-bitrate methods. HPC’s unique variable bitrate capabilities enable progressive streaming and rendering across various quality levels, making it particularly suitable for scenarios with fluctuations in bandwidth and computational resources. This provides a fundamental basis for the widespread application of volumetric video.

Acknowledgments

This work was supported by National Natural Science Foundation of China (62271308), STCSM (22511105700, 22DZ2229005), 111 plan (BP0719010), Open Project of National Key Laboratory of China

(23Z670104657) and State Key Laboratory of UHD Video and Audio Production and Presentation.

References

- [1] Eirikur Agustsson, Fabian Mentzer, Michael Tschannen, Lukas Cavigelli, Radu Timofte, Luca Benini, and Luc V Gool. 2017. Soft-to-hard vector quantization for end-to-end learning compressible representations. *Advances in neural information processing systems* 30 (2017).
- [2] Johannes Ballé, Valero Laparra, and Eero P Simoncelli. 2016. End-to-end optimization of nonlinear transform codes for perceptual quality. In *2016 Picture Coding Symposium (PCS)*. IEEE, 1–5.
- [3] Johannes Ballé, David Minnen, Saurabh Singh, Sung Jin Hwang, and Nick Johnston. 2018. Variational image compression with a scale hyperprior. In *6th International Conference on Learning Representations*.
- [4] Jonathan T. Barron, Ben Mildenhall, Matthew Tancik, Peter Hedman, Ricardo Martin-Brualla, and Pratul P. Srinivasan. 2021. Mip-NeRF: A Multiscale Representation for Anti-Aliasing Neural Radiance Fields. *ICCV* (2021).
- [5] Jonathan T. Barron, Ben Mildenhall, Dor Verbin, Pratul P. Srinivasan, and Peter Hedman. 2022. Mip-NeRF 360: Unbounded Anti-Aliased Neural Radiance Fields. *CVPR* (2022).
- [6] Jonathan T. Barron, Ben Mildenhall, Dor Verbin, Pratul P. Srinivasan, and Peter Hedman. 2023. Zip-NeRF: Anti-Aliased Grid-Based Neural Radiance Fields. *ICCV* (2023).
- [7] Ang Cao and Justin Johnson. 2023. HexPlane: A Fast Representation for Dynamic Scenes. In *Proceedings of the IEEE/CVF Conference on Computer Vision and Pattern Recognition (CVPR)*. 130–141.
- [8] Eric R Chan, Connor Z Lin, Matthew A Chan, Koki Nagano, Boxiao Pan, Shalini De Mello, Orazio Gallo, Leonidas J Guibas, Jonathan Tremblay, Sameh Khamis, et al. 2022. Efficient geometry-aware 3d generative adversarial networks. In *Proceedings of the IEEE/CVF conference on computer vision and pattern recognition*. 16123–16133.
- [9] Anpei Chen, Zexiang Xu, Andreas Geiger, Jingyi Yu, and Hao Su. 2022. Tensorf: Tensorial radiance fields. In *European Conference on Computer Vision*. Springer, 333–350.
- [10] Yu Chen and Gim Hee Lee. 2023. DBARF: Deep Bundle-Adjusting Generalizable Neural Radiance Fields. In *Proceedings of the IEEE/CVF Conference on Computer Vision and Pattern Recognition (CVPR)*. 24–34.
- [11] Zhiqin Chen, Thomas Funkhouser, Peter Hedman, and Andrea Tagliasacchi. 2023. Mobilenerf: Exploiting the polygon rasterization pipeline for efficient neural field rendering on mobile architectures. In *Proceedings of the IEEE/CVF Conference on Computer Vision and Pattern Recognition*. 16569–16578.
- [12] Zhibo Chen, Tianyu He, Xin Jin, and Feng Wu. 2020. Learning for Video Compression. *IEEE Transactions on Circuits and Systems for Video Technology* 30, 2 (2020), 566–576.
- [13] Wei Cheng, Ruixiang Chen, Siming Fan, Wanqi Yin, Keyu Chen, Zhongang Cai, Jingbo Wang, Yang Gao, Zhengming Yu, Zhengyu Lin, et al. 2023. Dna-rendering: A diverse neural actor repository for high-fidelity human-centric rendering. In *Proceedings of the IEEE/CVF International Conference on Computer Vision*. 19982–19993.
- [14] Jaesung Choe, Christopher Choy, Jaesik Park, In So Kweon, and Anima Anandkumar. 2023. Spacetime Surface Regularization for Neural Dynamic Scene Reconstruction. In *Proceedings of the IEEE/CVF International Conference on Computer Vision (ICCV)*. 17871–17881.
- [15] Chenxi Lola Deng and Enzo Tartaglione. 2023. Compressing explicit voxel grid representations: fast nerfs become also small. In *Proceedings of the IEEE/CVF Winter Conference on Applications of Computer Vision*. 1236–1245.
- [16] Yilun Du, Yinan Zhang, Hong-Xing Yu, Joshua B. Tenenbaum, and Jiajun Wu. 2021. Neural Radiance Flow for 4D View Synthesis and Video Processing. In *Proceedings of the IEEE/CVF International Conference on Computer Vision*.
- [17] Jiemin Fang, Taoran Yi, Xinggang Wang, Lingxi Xie, Xiaopeng Zhang, Wenyu Liu, Matthias Nießner, and Qi Tian. 2022. Fast Dynamic Radiance Fields with Time-Aware Neural Voxels. In *SIGGRAPH Asia 2022 Conference Papers (SA '22)*. ACM.
- [18] Sara Fridovich-Keil, Giacomo Meanti, Frederik Rahbæk Warburg, Benjamin Recht, and Angjoo Kanazawa. 2023. K-planes: Explicit radiance fields in space, time, and appearance. In *Proceedings of the IEEE/CVF Conference on Computer Vision and Pattern Recognition*. 12479–12488.
- [19] Sara Fridovich-Keil, Alex Yu, Matthew Tancik, Qinhong Chen, Benjamin Recht, and Angjoo Kanazawa. 2022. Plenoxels: Radiance fields without neural networks. In *Proceedings of the IEEE/CVF Conference on Computer Vision and Pattern Recognition*. 5501–5510.
- [20] Chen Gao, Ayush Saraf, Johannes Kopf, and Jia-Bin Huang. 2021. Dynamic View Synthesis from Dynamic Monocular Video. In *Proceedings of the IEEE International Conference on Computer Vision*.
- [21] Peter Hedman, Pratul P Srinivasan, Ben Mildenhall, Jonathan T Barron, and Paul Debevec. 2021. Baking neural radiance fields for real-time view synthesis. In *Proceedings of the IEEE/CVF International Conference on Computer Vision*. 5875–5884.
- [22] Mustafa Işık, Martin Rünz, Markos Georgopoulos, Taras Khakhulin, Jonathan Starck, Lourdes Agapito, and Matthias Nießner. 2023. HumanRF: High-Fidelity Neural Radiance Fields for Humans in Motion. *ACM Transactions on Graphics (TOG)* 42, 4 (2023).
- [23] Suyi Jiang, Haoran Jiang, Ziyu Wang, Haimin Luo, Wenzheng Chen, and Lan Xu. 2023. Humangen: Generating human radiance fields with explicit priors. In *Proceedings of the IEEE/CVF Conference on Computer Vision and Pattern Recognition*. 12543–12554.
- [24] Kyungmin Jo, Gyumin Shim, Sanghun Jung, Soyoung Yang, and Jaegul Choo. 2023. CG-NeRF: Conditional generative neural radiance fields for 3D-aware image synthesis. In *Proceedings of the IEEE/CVF Winter Conference on Applications of Computer Vision*. 724–733.
- [25] Nick Johnston, Damien Vincent, David Minnen, Michele Covell, Saurabh Singh, Troy Chinen, Sung Jin Hwang, Joel Shor, and George Toderici. 2018. Improved lossy image compression with priming and spatially adaptive bit rates for recurrent networks. In *Proceedings of the IEEE conference on computer vision and pattern recognition*. 4385–4393.
- [26] Fatih Kamisli, Fabien Racape, and Hyomin Choi. 2024. Variable-Rate Learned Image Compression with Multi-Objective Optimization and Quantization-Reconstruction Offsets. *arXiv preprint arXiv:2402.18930* (2024).
- [27] Seung Wook Kim, Bradley Brown, Kangxue Yin, Karsten Kreis, Katja Schwarz, Daiqing Li, Robin Rombach, Antonio Torralba, and Sanja Fidler. 2023. NeuralField-LDM: Scene Generation With Hierarchical Latent Diffusion Models. In *Proceedings of the IEEE/CVF Conference on Computer Vision and Pattern Recognition (CVPR)*. 8496–8506.
- [28] Soonbin Lee, Fangwen Shu, Yago Sanchez, Thomas Schierl, and Cornelius Hellge. 2023. ECRF: Entropy-Constrained Neural Radiance Fields Compression with Frequency Domain Optimization. *arXiv preprint arXiv:2311.14208* (2023).
- [29] Lingzhi Li, Zhen Shen, Zhongshu Wang, Li Shen, and Liefeng Bo. 2023. Compressing volumetric radiance fields to 1 mb. In *Proceedings of the IEEE/CVF Conference on Computer Vision and Pattern Recognition*. 4222–4231.
- [30] Lingzhi Li, Zhen Shen, Zhongshu Wang, Li Shen, and Ping Tan. 2022. Streaming radiance fields for 3d video synthesis. *Advances in Neural Information Processing Systems* 35 (2022), 13485–13498.
- [31] Mu Li, Wangmeng Zuo, Shuhang Gu, Debin Zhao, and David Zhang. 2018. Learning Convolutional Networks for Content-Weighted Image Compression. In *2018 IEEE/CVF Conference on Computer Vision and Pattern Recognition*. 3214–3223.
- [32] Tianye Li, Mira Slavcheva, Michael Zollhoefer, Simon Green, Christoph Lassner, Changil Kim, Tanner Schmidt, Steven Lovegrove, Michael Goesele, Richard Newcombe, et al. 2022. Neural 3d video synthesis from multi-view video. In *Proceedings of the IEEE/CVF Conference on Computer Vision and Pattern Recognition*. 5521–5531.
- [33] Zhaoshuo Li, Thomas Müller, Alex Evans, Russell H Taylor, Mathias Unberath, Ming-Yu Liu, and Chen-Hsuan Lin. 2023. Neuralangelo: High-Fidelity Neural Surface Reconstruction. In *IEEE Conference on Computer Vision and Pattern Recognition (CVPR)*.
- [34] Chen-Hsuan Lin, Wei-Chiu Ma, Antonio Torralba, and Simon Lucey. 2021. Barf: Bundle-adjusting neural radiance fields. In *Proceedings of the IEEE/CVF International Conference on Computer Vision*. 5741–5751.
- [35] Kai Lin, Chuanmin Jia, Xinfeng Zhang, Shanshe Wang, Siwei Ma, and Wen Gao. 2023. DMVC: Decomposed Motion Modeling for Learned Video Compression. *IEEE Transactions on Circuits and Systems for Video Technology* 33, 7 (2023), 3502–3515.
- [36] Haojie Liu, Tong Chen, Peiyao Guo, Qiu Shen, Xun Cao, Yao Wang, and Zhan Ma. 2019. Non-local Attention Optimized Deep Image Compression.
- [37] Jia-Wei Liu, Yan-Pei Cao, Weijia Mao, Wenqiao Zhang, David Junhao Zhang, Jussi Keppo, Ying Shan, Xiaohu Qie, and Mike Zheng Shou. 2022. Devrf: Fast deformable voxel radiance fields for dynamic scenes. *Advances in Neural Information Processing Systems* 35 (2022), 36762–36775.
- [38] Xiaoxiao Long, Cheng Lin, Lingjie Liu, Yuan Liu, Peng Wang, Christian Theobalt, Taku Komura, and Wenping Wang. 2023. NeuralUDF: Learning Unsigned Distance Fields for Multi-View Reconstruction of Surfaces With Arbitrary Topologies. In *Proceedings of the IEEE/CVF Conference on Computer Vision and Pattern Recognition (CVPR)*. 20834–20843.
- [39] Guo Lu, Wanli Ouyang, Dong Xu, Xiaoyun Zhang, Chunlei Cai, and Zhiyong Gao. 2019. DVC: An End-To-End Deep Video Compression Framework. In *2019 IEEE/CVF Conference on Computer Vision and Pattern Recognition (CVPR)*. 10998–11007.
- [40] Haichuan Ma, Dong Liu, Ning Yan, Houqiang Li, and Feng Wu. 2022. End-to-End Optimized Versatile Image Compression With Wavelet-Like Transform. *IEEE Transactions on Pattern Analysis and Machine Intelligence* 44, 3 (2022), 1247–1263.
- [41] Jue Mao and Lu Yu. 2020. Convolutional Neural Network Based Bi-Prediction Utilizing Spatial and Temporal Information in Video Coding. *IEEE Transactions on Circuits and Systems for Video Technology* 30, 7 (2020), 1856–1870.
- [42] G Nigel N Martin. 1979. Range encoding: an algorithm for removing redundancy from a digitised message. In *Proc. Institution of Electronic and Radio Engineers*

- International Conference on Video and Data Recording*, Vol. 2.
- [43] Ricardo Martin-Brualla, Noha Radwan, Mehdi S. M. Sajjadi, Jonathan T. Barron, Alexey Dosovitskiy, and Daniel Duckworth. 2021. NeRF in the Wild: Neural Radiance Fields for Unconstrained Photo Collections. In *CVPR*.
- [44] Xiandong Meng, Chen Chen, Shuyuan Zhu, and Bing Zeng. 2018. A New HEVC In-Loop Filter Based on Multi-channel Long-Short-Term Dependency Residual Networks. In *2018 Data Compression Conference*. 187–196.
- [45] Gal Metzger, Elad Richardson, Or Patashnik, Raja Giryes, and Daniel Cohen-Or. 2023. Latent-nerf for shape-guided generation of 3d shapes and textures. In *Proceedings of the IEEE/CVF Conference on Computer Vision and Pattern Recognition*. 12663–12673.
- [46] Ben Mildenhall, Pratul P Srinivasan, Matthew Tancik, Jonathan T Barron, Ravi Ramamoorthi, and Ren Ng. 2021. Nerf: Representing scenes as neural radiance fields for view synthesis. *Commun. ACM* 65, 1 (2021), 99–106.
- [47] Thomas Müller, Alex Evans, Christoph Schied, and Alexander Keller. 2022. Instant Neural Graphics Primitives with a Multiresolution Hash Encoding. *ACM Trans. Graph.* 41, 4, Article 102 (July 2022), 15 pages.
- [48] Keunhong Park, Utkarsh Sinha, Jonathan T. Barron, Sofien Bouaziz, Dan B Goldman, Steven M. Seitz, and Ricardo Martin-Brualla. 2021. Nerfies: Deformable Neural Radiance Fields. In *Proceedings of the IEEE/CVF International Conference on Computer Vision (ICCV)*. 5865–5874.
- [49] Philipp Mildenhall Ben; Barron Jonathan T.; Martin-Brualla Ricardo Park, Keunhong; Henzler. 2023. CamP: Camera Preconditioning for Neural Radiance Fields. *ACM Trans. Graph.* (2023).
- [50] By S Pateux and J. Jung. 2007. An Excel add-in for computing Bjontegaard metric and its evolution.," in VCEG Meeting. (2007).
- [51] Sida Peng, Yunzhi Yan, Qing Shuai, Hujun Bao, and Xiaowei Zhou. 2023. Representing volumetric videos as dynamic mlp maps. In *Proceedings of the IEEE/CVF Conference on Computer Vision and Pattern Recognition*. 4252–4262.
- [52] Albert Pumarola, Enric Corona, Gerard Pons-Moll, and Francesc Moreno-Noguer. 2020. D-NeRF: Neural Radiance Fields for Dynamic Scenes. In *Proceedings of the IEEE/CVF Conference on Computer Vision and Pattern Recognition*.
- [53] Saskia Rabich, Patrick Stotko, and Reinhard Klein. 2023. FPO++: Efficient Encoding and Rendering of Dynamic Neural Radiance Fields by Analyzing and Enhancing Fourier Plenotrees. *arXiv preprint arXiv:2310.20710* (2023).
- [54] Christian Reiser, Rick Szeliski, Dor Verbin, Pratul Srinivasan, Ben Mildenhall, Andreas Geiger, Jon Barron, and Peter Hedman. 2023. Merf: Memory-efficient radiance fields for real-time view synthesis in unbounded scenes. *ACM Transactions on Graphics (TOG)* 42, 4 (2023), 1–12.
- [55] Daniel Rho, Byeonghyeon Lee, Seungtae Nam, Joo Chan Lee, Jong Hwan Ko, and Eunbyung Park. 2023. Masked Wavelet Representation for Compact Neural Radiance Fields. In *Proceedings of the IEEE/CVF Conference on Computer Vision and Pattern Recognition*. 20680–20690.
- [56] Sara Rojas, Jesus Zarzar, Juan C Pérez, Artsiom Sanakoyeu, Ali Thabet, Albert Pumarola, and Bernard Ghanem. 2023. Re-rem: Real-time rendering of nerfs across devices. In *Proceedings of the IEEE/CVF International Conference on Computer Vision*. 3632–3641.
- [57] Ruizhi Shao, Zerong Zheng, Hanzhang Tu, Boning Liu, Hongwen Zhang, and Yebin Liu. 2023. Tensor4d: Efficient neural 4d decomposition for high-fidelity dynamic reconstruction and rendering. In *Proceedings of the IEEE/CVF Conference on Computer Vision and Pattern Recognition*. 16632–16642.
- [58] Xihua Sheng, Jiahao Li, Bin Li, Li Li, Dong Liu, and Yan Lu. 2023. Temporal Context Mining for Learned Video Compression. *IEEE Transactions on Multimedia* 25 (2023), 7311–7322.
- [59] Liangchen Song, Anpei Chen, Zhong Li, Zhang Chen, Lele Chen, Junsong Yuan, Yi Xu, and Andreas Geiger. 2023. Nerfplayer: A streamable dynamic scene representation with decomposed neural radiance fields. *IEEE Transactions on Visualization and Computer Graphics* 29, 5 (2023), 2732–2742.
- [60] Jiayang Tang, Xiaokang Chen, Jingbo Wang, and Gang Zeng. 2022. Compressible-composable nerf via rank-residual decomposition. *Advances in Neural Information Processing Systems* 35 (2022), 14798–14809.
- [61] Jiayang Tang, Hang Zhou, Xiaokang Chen, Tianshu Hu, Errui Ding, Jingdong Wang, and Gang Zeng. 2023. Delicate textured mesh recovery from nerf via adaptive surface refinement. In *Proceedings of the IEEE/CVF International Conference on Computer Vision*. 17739–17749.
- [62] Lucas Theis, Wenzhe Shi, Andrew Cunningham, and Ferenc Huszár. 2016. Lossy image compression with compressive autoencoders. In *International Conference on Learning Representations*.
- [63] George Toderici, Damien Vincent, Nick Johnston, Sung Jin Hwang, David Minnen, Joel Shor, and Michele Covell. 2017. Full resolution image compression with recurrent neural networks. In *Proceedings of the IEEE conference on Computer Vision and Pattern Recognition*. 5306–5314.
- [64] Hengyi Wang, Jingwen Wang, and Lourdes Agapito. 2023. Co-SLAM: Joint Coordinate and Sparse Parametric Encodings for Neural Real-Time SLAM. In *Proceedings of the IEEE/CVF Conference on Computer Vision and Pattern Recognition (CVPR)*. 13293–13302.
- [65] Liao Wang, Qiang Hu, Qihan He, Ziyu Wang, Jingyi Yu, Tinne Tuytelaars, Lan Xu, and Minye Wu. 2023. Neural Residual Radiance Fields for Streamably Free-Viewpoint Videos. In *Proceedings of the IEEE/CVF Conference on Computer Vision and Pattern Recognition (CVPR)*. 76–87.
- [66] Liao Wang, Kaixin Yao, Chengcheng Guo, Zhirui Zhang, Qiang Hu, Jingyi Yu, Lan Xu, and Minye Wu. 2023. VideoRF: Rendering Dynamic Radiance Fields as 2D Feature Video Streams.
- [67] Liao Wang, Jiakai Zhang, Xinhang Liu, Fuqiang Zhao, Yanshun Zhang, Yingliang Zhang, Minye Wu, Jingyi Yu, and Lan Xu. 2022. Fourier plenotrees for dynamic radiance field rendering in real-time. In *Proceedings of the IEEE/CVF Conference on Computer Vision and Pattern Recognition*. 13524–13534.
- [68] Peng Wang, Lingjie Liu, Yuan Liu, Christian Theobalt, Taku Komura, and Wenping Wang. 2021. NeuS: Learning Neural Implicit Surfaces by Volume Rendering for Multi-view Reconstruction. In *Proc. Advances in Neural Information Processing Systems (NeurIPS)*, Vol. 34. 27171–27183.
- [69] Yiming Wang, Qin Han, Marc Habermann, Kostas Daniilidis, Christian Theobalt, and Lingjie Liu. 2023. NeuS2: Fast Learning of Neural Implicit Surfaces for Multi-view Reconstruction. In *Proceedings of the IEEE/CVF International Conference on Computer Vision (ICCV)*.
- [70] Minye Wu, Yuehao Wang, Qiang Hu, and Jingyi Yu. 2020. Multi-view neural human rendering. In *Proceedings of the IEEE/CVF Conference on Computer Vision and Pattern Recognition*. 1682–1691.
- [71] Minye Wu, Zehao Wang, Georgios Kouros, and Tinne Tuytelaars. 2023. TeTriRF: Temporal Tri-Plane Radiance Fields for Efficient Free-Viewpoint Video. *arXiv preprint arXiv:2312.06713* (2023).
- [72] W. Xian, J. Huang, J. Kopf, and C. Kim. 2021. Space-time Neural Irradiance Fields for Free-Viewpoint Video. In *2021 IEEE/CVF Conference on Computer Vision and Pattern Recognition (CVPR)*. IEEE Computer Society, Los Alamitos, CA, USA, 9416–9426.
- [73] Ning Yan, Dong Liu, Houqiang Li, Bin Li, Li Li, and Feng Wu. 2019. Invertibility-Driven Interpolation Filter for Video Coding. *IEEE Transactions on Image Processing* 28, 10 (2019), 4912–4925.
- [74] R. Yang, M. Xu, Z. Wang, and T. Li. 2018. Multi-frame Quality Enhancement for Compressed Video. In *2018 IEEE/CVF Conference on Computer Vision and Pattern Recognition (CVPR)*. Los Alamitos, CA, USA, 6664–6673.
- [75] Lior Yariv, Peter Hedman, Christian Reiser, Dor Verbin, Pratul P Srinivasan, Richard Szeliski, Jonathan T Barron, and Ben Mildenhall. 2023. Bakedsd: Meshing neural sdfs for real-time view synthesis. In *ACM SIGGRAPH 2023 Conference Proceedings*. 1–9.
- [76] Heng Yu, Joel Julin, Zoltán Á. Milacski, Koichiro Niinuma, and László A. Jeni. 2023. DyLiN: Making Light Field Networks Dynamic. In *Proceedings of the IEEE/CVF Conference on Computer Vision and Pattern Recognition (CVPR)*. 12397–12406.
- [77] Shiran Yuan and Hao Zhao. 2023. SlimmerRF: Slimmable Radiance Fields. *arXiv preprint arXiv:2312.10034* (2023).
- [78] Anlan Zhang, Chendong Wang, Bo Han, and Feng Qian. 2022. YuZu: Neural-Enhanced Volumetric Video Streaming. In *19th USENIX Symposium on Networked Systems Design and Implementation (NSDI 22)*. USENIX Association, Renton, WA, 137–154.
- [79] Zhiyu Zhang, Guo Lu, Huanxiong Liang, Anni Tang, Qiang Hu, and Li Song. 2024. Efficient Dynamic-NeRF Based Volumetric Video Coding with Rate Distortion Optimization. *arXiv preprint arXiv:2402.01380* (2024).
- [80] Zhenghui Zhao, Shiqi Wang, Shanshe Wang, Xinfeng Zhang, Siwei Ma, and Jian-sheng Yang. 2019. Enhanced Bi-Prediction With Convolutional Neural Network for High-Efficiency Video Coding. *IEEE Transactions on Circuits and Systems for Video Technology* 29, 11 (2019), 3291–3301.
- [81] Zihan Zheng, Houqiang Zhong, Qiang Hu, Xiaoyun Zhang, Li Song, Ya Zhang, and Yanfeng Wang. 2024. JointRF: End-to-End Joint Optimization for Dynamic Neural Radiance Field Representation and Compression. *arXiv preprint arXiv:2405.14452* (2024).
- [82] Zihan Zhu, Songyou Peng, Viktor Larsson, Zhaopeng Cui, Martin R Oswald, Andreas Geiger, and Marc Pollefeys. 2024. NICER-SLAM: Neural Implicit Scene Encoding for RGB SLAM. In *International Conference on 3D Vision (3DV)*.
- [83] Zihan Zhu, Songyou Peng, Viktor Larsson, Weiwei Xu, Hujun Bao, Zhaopeng Cui, Martin R Oswald, and Marc Pollefeys. 2022. Nice-slam: Neural implicit scalable encoding for slam. In *Proceedings of the IEEE/CVF Conference on Computer Vision and Pattern Recognition*. 12786–12796.

A More Qualitative Results

The enhanced rendering outcomes from our HPC framework applied to the ReRF[65] and DNA-Rendering[13] datasets are shown in Fig. A1. They further demonstrate the effectiveness of our method across diverse datasets. Additionally, this showcases our method's capability to support variable bitrate streaming within a single model.



Figure A1: The rendered outcomes of our HPC framework on different datasets.

B Progressive Training Strategy

A detailed exposition of the progressive training strategy is presented in Algorithm.(1).

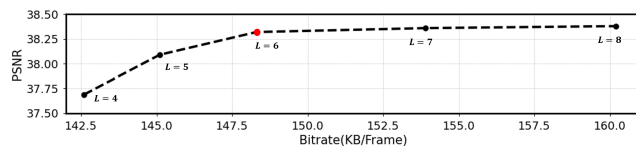
C More Detailed Configurations

In all comparative experiments, we set the bounding boxes for the entire DNA dataset to $[[[-0.7, -0.2, -0.7], [0.7, 1.55, 0.7]]]$. For the ReRF dataset, the bounding boxes were set as follows: the kpop sequence to $[[[-0.6, -0.5, -1.25], [0.6, 0.7, 0.1]]]$, the box sequence to $[[[-0.55, -0.5, -1.18], [0.55, 0.55, 0]]]$, and the sing sequence to $[[[-0.85, -0.5, -1.15], [0.35, 0.3, 0.1]]]$.

To ensure fairness, all manual post-rendering adjustments to the background based on masks were prohibited, and the resolution of the generated images was set to match that of the input.

D Choice of L

To find the best value of L , we conducted additional experiments with different values of L . For $L > 6$, the quality gains are almost negligible but the model size continues increasing. Therefore, we selected $L = 6$ as the optimal choice.



Algorithm 1 Progressive Training Strategy

- 1: Initialize residual feature grids $R_t^1, R_t^2, \dots, R_t^L$
- 2: Initialize learning parameters λ_1, λ_2 , set maximum iterations $maxiter$, and active iteration step $actiter$
- 3: Get $\hat{F}_{t-1}^1, \hat{F}_{t-1}^2, \dots, \hat{F}_{t-1}^L$ from the reference frame buffer
- 4: Fix higher resolution grids $R_t^2, R_t^3, \dots, R_t^L$
- 5: Start training on R_t^1 with initial low-resolution
- 6: **for** $it \leftarrow 1$ to $maxiter$ **do**
- 7: **if** $it == l \times actiter$ **then**
- 8: Start gradient backpropagation for R_t^{l+1}
- 9: Begin entropy estimation and simulate quantization on R_t^{l+1}
- 10: **end if**
- 11: **if** $it == maxiter - l \times actiter$ **then**
- 12: Stop training on R_t^{l-1}
- 13: **if** current frame is keyframe **then**
- 14: Set $\lambda_1, \lambda_2 \leftarrow 0$ for refining the training focus
- 15: **end if**
- 16: **end if**
- 17: Update learning rates and regularization parameters dynamically
- 18: Combine activated R_t^l with corresponding \hat{F}_{t-1}^l to get \hat{F}_t^l
- 19: Calculate the corresponding L^l and perform gradient backpropagation
- 20: **end for**
- 21: Put well-trained \hat{F}_t into the reference frame buffer